Environmental Science
Water Research & Technology

ROYAL SOCIETY OF CHEMISTRY

PAPER

View Article Online
View Journal

Cite this: DOI: 10.1039/d5ew00977d

Desaturation and chemical recovery from desalination concentrates using ion exchange and bipolar membrane electrodialysis as a zero liquid discharge process

Luis Salas, *[ab] Alex Schwarz [b] and Alvaro Gonzalez-Vogel [a]

Received 5th October 2025,
Accepted 2nd December 2025

DOI: 10.1039/d5ew00977d

rsc.li/es-water

The cellulose pulp industry still consumes high amounts of water, making water recovery essential. To address this, pulsed electrodialysis reversal (pEDR) has been proposed; however, the remaining concentrate management is still a challenge. Thus, this study evaluates an integrated system combining ion exchange, pEDR and bipolar membrane electrodialysis for concentrate desaturation and simultaneous recovery of caustics and acids, as an alternative to conventional zero liquid discharge systems, such as evaporation and crystallization. Experiments with ion exchange resins assessed their capacity with industrial effluents, while bipolar membrane electrodialysis was tested at different voltages and (synthetic) reject stream concentrations. A nine-step setup simulated industrial performance, achieving 0.67 M NaOH with 73% efficiency and an energy consumption of 4.57 kWh kg^{-1} NaOH. Economic analysis showed that integrating pEDR with evaporation and crystallization in an industrial scale system requires nearly 38% more in capital cost than integrating pEDR with the desaturation system. The operational cost for evaporation–crystallization with pEDR is 0.43 USD per m^3, while desaturation with pEDR costs 0.34 USD per m^3 and decreases to 0.20 USD per m^3 with soda valorization. These results show a more sustainable and cost-effective alternative for zero liquid discharge in the cellulose pulp industry.

Water impact

This study demonstrates a cost-effective alternative to conventional zero liquid discharge systems in pulp mills, reducing capital costs by 38% and operational costs by up to 53% through chemical recovery. The integrated pulsed electrodialysis and bipolar membrane system enables water recycling while converting waste streams into reusable caustics and acids, advancing circular economy principles in water-intensive industries.

1. Introduction

The cellulose pulp industry is a key global sector, producing items like toilet paper, printing paper, and packaging. Globalization has driven major changes, increasing competition and output, especially in Asia and South America.[5] Pulp production rose from 120 million tons in 1982 to nearly 190 million in 2021.[9]

A major environmental concern is high-water consumption and liquid discharge. Bleaching is the most water-intensive stage, consuming up to 50% of a plant's water and generating 80% of its effluent,[24,28] due to pulp washing after each step to remove oxidized materials.[23] A kraft pulp mill producing one million tons annually consumes water comparable to a city of 500 000 habitants.[22] Efficiency improvements have reduced water consumption from 200 m^3 per ton of air-dry pulp (ADt) in the 1960s to below 25 m^3 ADt^{-1} in modern mills.[18] However, further reductions remain challenging and costly, especially when closing water loops.

Desalination technologies such as evaporation, reverse osmosis and electrodialysis are commercially available on a large scale[14] but are unsuitable for pulp mill effluents. Evaporation is highly energy-intensive, while membrane-based processes suffer from organic and inorganic fouling. As an alternative, variations of electrodialysis, such as electrodialysis reversal (EDR)[1] and pulsed electrodialysis,[13] have been proposed. EDR reduces the need for pretreatment and cleaning-in-place procedures compared to conventional electrodialysis, but this is achieved at the expense of lower production rates. On the other hand, in pulsed electrodialysis, membrane fouling remains a significant issue, limiting its viability by reducing process efficiency and

[a] Bioforest SpA, Camino Coronel Km 15, Coronel, 4190000, Chile
[b] Department of Civil Engineering, Universidad de Concepción, P.O. Box 160-C, Concepción, 4030000, Chile. E-mail: lusalas@udec.cl

membrane lifespan.[1] A promising solution to these limitations is pulsed electrodialysis reversal (pEDR),[14] which has been proposed as a key technology to at least partially close the water loop in bleached kraft pulp mills.

Although pEDR maximizes water recovery, the concentrate loop accumulates inorganic and organic ions that must be removed. Typically, reject is recirculated near saturation, with make-up water added to prevent exceeding solubility limits. Some of the concentrate is discharged, but due to its high salinity, discharge could be restricted, making its treatment a significant challenge.

The most used concentrate treatment is evaporation/crystallization, a zero liquid discharge (ZLD) method that recovers water and produces solid salts *via* thermal processes. However, this method is energy-intensive and costly, and lacks circularity. To address this, we investigate bipolar membrane electrodialysis (BMED) to desaturate the concentrate and ion exchange (IX) as a pretreatment to protect the membranes (Fig. 1). BMED shows potential in ZLD and resource recovery due to its unique membrane structure,[42] consisting of cation/anion exchange layers and an interfacial layer.[25] Under direct current fields, water in the interfacial layer splits into H^+ and OH^- ions,[20] enabling salt conversion into acids and caustics without chemicals, reducing pollution and generating valuable by-products.[30]

However, BMED performance can be adversely affected by contaminants, such as organic matter and multivalent metal ions. Organic pollutants in pulp effluents include carbohydrates, extractives, lignans, lignin-derived phenolics, and low molecular weight acids.[32] Humic and fulvic acids and other lignin derivatives are also present.[27] Here, we proposed for the first time pEDR as a pretreatment stage of bipolar membranes, as most of the organics in the effluents cannot cross the ion exchange membranes of electrodialysis. On the other hand, the problematic multivalent metal ions are hardness ions Ca^{2+} and Mg^{2+} which can form precipitates, blocking cation exchange membranes, increasing electrical resistance, and reducing efficiency and equipment lifetime.[39,43] IX columns effectively remove hardness ions by exchanging them with resin-bound ions.[19] IX is highly selective and efficient at removing metal ions, even at low concentrations.[26] To complete the loop, IX regeneration stream, rich in calcium and magnesium, can be treated by chemical precipitation. Magnesium and calcium hydroxides can be selectively precipitated by adding alkaline solution in two consecutive steps while controlling the pH.[37] These ions are valuable for the forestry industry and can be recycled to the forests if necessary.

This research evaluates an alternative ZLD system to traditional evaporation and crystallization in the kraft pulp industry based on IX as a pretreatment, pEDR as an isolation stage and BMED for desaturation of concentrates. The proposed technologies are evaluated experimentally and compared to conventional solutions in terms of performance, costs and sustainability.

2. Materials and methods

2.1 Characterization of the solutions

The schematic of the proposed solution is illustrated in Fig. 1, integrating pEDR desalination, IX pretreatment and BMED desaturation. Here, we evaluate IX and BMED, since pEDR desalination was already evaluated in ref. 14.

For the IX pretreatment, the influent stream corresponds to the tertiary effluent from the pulp mill, previously treated using conventional methods. Tertiary effluent and pEDR (2 stages) dilute characterization results are presented in Table 1. Samples correspond to data obtained from the operation of a pEDR pilot plant. The pulp mill effluent refers to the characterization after ultrafiltration and before pEDR.

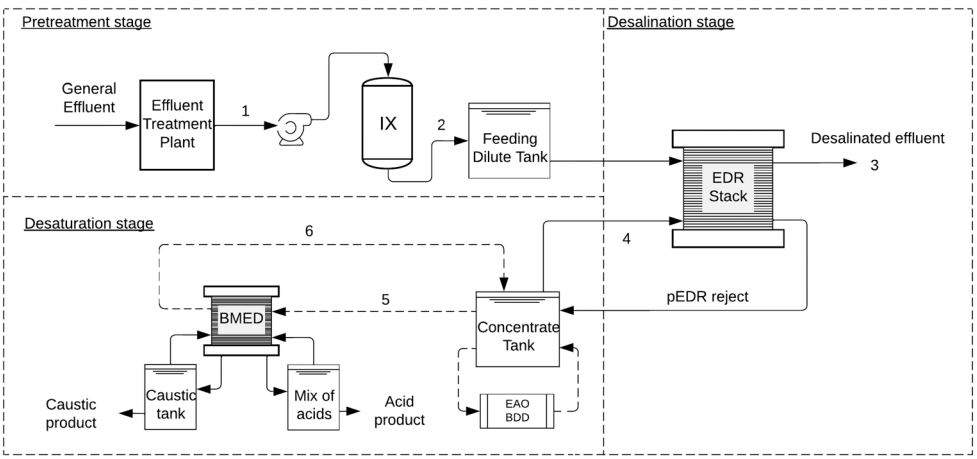

Fig. 1 Flow representation of the water treatment process for kraft pulp mill effluent. (1) Tertiary effluent from the pulp mill after conventional treatment, (2) softened effluent by IX as a pretreatment unit to pEDR and BMED to prevent scaling. The softened effluent is then processed by pEDR, resulting in (3) desalinated effluent, which is returned to the pulp mill, and pEDR reject. A portion of the reject is recirculated (4) and the other is purged (5) and sent to the desaturation stage, where the concentrate is treated by BMED, generating desaturated concentrate (6). In this stage, electrochemical advanced-oxidation using boron-doped diamond (BDD) anodes is also proposed as an alternative for organic load desaturation when required.

Table 1 Characterization of the pulp mill effluent and pEDR dilute. Mean value and standard deviation

Parameter	Pulp mill effluent	pEDR dilute	Unit
Aluminum	0.04 ± 0.02	0.045 ± 0.026	mg l^{-1}
Calcium	3.89 ± 2.78	0.42 ± 0.85	mg l^{-1}
Chloride	63.71 ± 25.62	6.74 ± 4.013	mg l^{-1}
COD	31.22 ± 7.59	24.78 ± 10.61	mg l^{-1}
Iron	0.018 ± 0.006	0.018 ± 0.011	mg l^{-1}
Magnesium	1.10 ± 0.41	0.083 ± 0.078	mg l^{-1}
Manganese	0.003 ± 0.0019	<0.002	mg l^{-1}
Potassium	5.15 ± 2.69	2.40 ± 2.86	mg l^{-1}
Silica	8.51 ± 4.03	10.58 ± 1.36	mg l^{-1}
Sodium	91.64 ± 45.75	34.74 ± 17.84	mg l^{-1}
Sulfate	138.05 ± 65.68	51.59 ± 20.26	mg l^{-1}
Conductivity	665.67 ± 235.16	157.57 ± 49.78	mS cm^{-1}
pH	7.44 ± 0.43	6.11 ± 0.27	–

The data correspond to a 45 day discontinuous operation period, with a total of 18 measurements for each parameter.

In BMED experiments, a synthetic solution of pEDR concentrate was prepared, considering the main salts identified through the characterization of the concentrate in the pilot test (NaCl and Na_2SO_4) as they account for more than 85% of the total dissolved solids in the effluent. To evaluate the salt concentration effect on BMED performance, we tested three different synthetic solutions within the concentrate operational range observed in the pilot tests. These solutions are presented in Table 2.

2.2 Experimental procedures

2.2.1 Ion exchange experiments and modelling of chemical precipitation. IX tests were conducted using LEWATIT MonoPlus TP 207, a weak acid resin in its sodium form with an exchange capacity of 2.0 eq l^{-1}. A column operation was performed to evaluate the saturation curve of a fixed bed. A Plexiglass© column with an internal diameter of 2.5 cm and a height of 16 cm was used. The resin bed height was set at 4 cm to reduce the experiment duration. Polyurethane foam was placed at the top of the bed to ensure a uniform distribution of the feed, while a 6 mm diameter glass bead (Merck, cat. no. 104018) was used at the bottom to prevent resin loss. The tertiary effluent was obtained from the plant and fed into the column at an average flow rate of 22 bed volumes (BV) per hour, controlled using a Masterflex L/S Easy-Load II peristaltic pump. The working temperature ranged from 26 °C to 29 °C, based on historical data of the pulp mill's effluent temperature (27.33 ± 0.97). Samples were collected every 0.2 BV until reaching 1 BV of the treated effluent volume to verify appropriate resin performance.

Table 2 Characterization of the simulated pEDR concentrate for BMED

Conductivity (mS cm^{-1})	NaCl [mM]	Na_2SO_4 [mM]
10	42.5	42.7
14	62.5	62.7
18	82.5	82.7

Then, samples were taken every 6 BV and kept in a cold chamber. Measurements were performed at different BV values until the breakpoint was reached. The experiment was stopped when the outlet concentration exceeded the breakpoint, which, in this study, was defined as 10% of the inlet concentration. The concentration of calcium and magnesium was determined by means of an optical emission spectrometer (ICP-OES Agilent 5800). Finally, the resin capacity Q_{tb} (eq l^{-1}) up to the time of the breaking point was calculated as follows:

$$Q_{tb} = \frac{V_b \cdot (C_o - C_{tb})}{V_r} \quad (1)$$

where V_b is the volume (L) of the effluent that passed through the column until the breakpoint, C_o is the feed hardness concentration (eq l^{-1}), C_{tb} is the effluent hardness concentration (eq L^{-1}), and V_r is the volume (L) occupied by the resin in the column. The IX regeneration stream was characterized through modeling in Water Application Value Engine (WAVE).[8] The chemical precipitation of this stream was modeled in PHREEQC,[36] first considering the reaction with sodium hydroxide (NaOH) for the precipitation of magnesium hydroxide, followed by the reaction with sodium carbonate (Na_2CO_3) for the precipitation of calcium carbonate.

2.2.2 BMED experiments. PCCell ED-64004 BMED equipment (PCCell GmbH, Germany) was used, consisting in this case of a three-chamber system with an effective membrane area of 64 cm^2 for each membrane. The setup included four membrane triplets, each composed of a cation membrane (membrane type: CMB), an anionic membrane (membrane type: AHA) and a bipolar membrane (membrane type: BPM), with a total bipolar membrane area of 256 cm^2. All membranes were purchased from Ameridia (USA). Additionally, an extra cationic membrane was placed at the anode end to compensate for the cation losses in the final compartment near the cathode. As a result, a total of five cationic membranes, four anionic membranes, and four bipolar membranes were used. The membrane properties are shown in Table 3. The cell configuration along with the laboratory setup is illustrated in Fig. 2.

The experiments were conducted under constant voltage (potentiostatic mode) across the electrodes. Four pumps controlled the flow in the BMED system. The flow rate in the three compartments (salt, acid and base) was maintained at a constant value of 10 L h^{-1} for all experiments, while the electrode flow rate was set at 30 L h^{-1}. Throughout the experiments, the temperature, conductivity, voltage and current were constantly measured in all three compartments. Additionally, for the acid compartment, the pH was constantly measured. The temperature was maintained in the same range of IX, 26 °C to 29 °C, with a water jacket in all the compartments, according to the data obtained from the pulp mill effluent. The experiments were conducted over the range of 10 mS cm^{-1} to 2 mS cm^{-1}, 14 mS cm^{-1} to 6.30 mS

Table 3 Properties of utilized ASTOM membranes

	Type	Electrical resistance (Ω cm^{-2})	Membrane thickness (mm)	Thermal stability (°C)	pH	Burst strength (MPa)
CMB	Cation exchange	4.5	0.21	≤60	0–14	≥0.40
AHA	Anion exchange	4.1	0.22	≤60	0–14	≥0.90
BP-1	Bipolar membrane	—	0.28	—	—	≥0.70

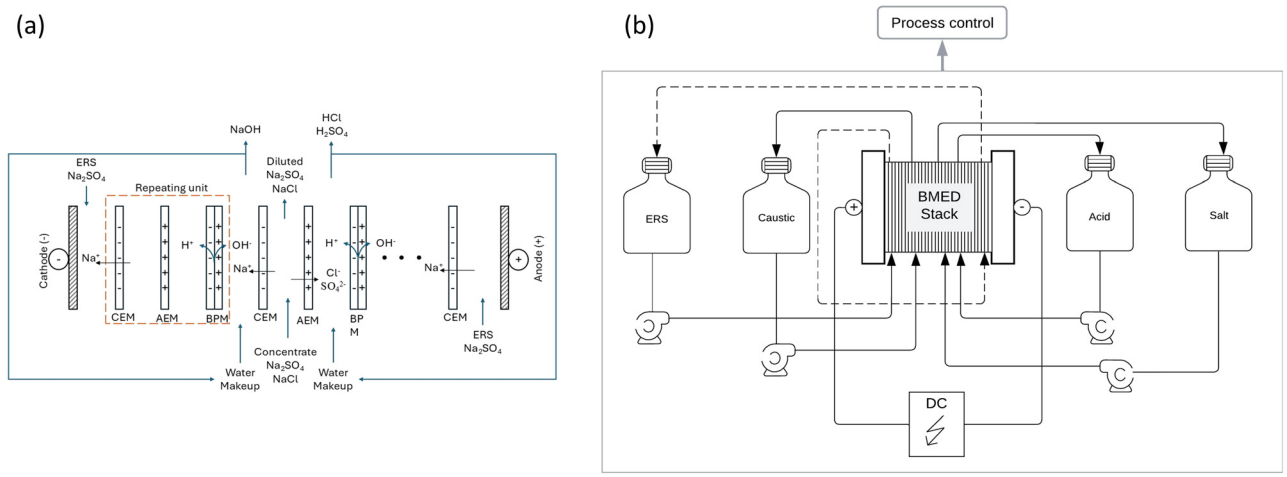

Fig. 2 (a) Schematic diagram of BMED arrangement inside the cell. Cathode (–) on the left side and anode (+) on the right side. The dotted square represents the repetitive units, consisting of a cation exchange membrane (CEM), an anion exchange membrane (AEM), and a bipolar membrane (BPM). Additionally, a final cation exchange membrane was used. (b) Representation of the BMED laboratory equipment. The system includes the BMED stack, a direct current (DC) power supply, and containers for acid, soda, salt solution and electrode rinse solution (ERS), equipped with their respective pump.

cm^{-1}, and 18 mS cm^{-1} to 9.90 mS cm^{-1}, to achieve the required desaturation rate.

Energy consumption (Ec, kWh kg^{-1} NaOH) and current efficiency (Ie, %) were calculated using eqn (2) and (3), respectively, as described by ref. 33. The desaturation rate was calculated using eqn (4).

$$\mathrm{Ec} = \int \frac{(UI_t \mathrm{d}t)}{(C_t V_t - C_0 V_0) M} \tag{2}$$

$$\mathrm{Ie} = \frac{z \cdot (V_t \cdot C_t - V_0 \cdot C_0) F}{NIt} \tag{3}$$

$$\text{Desaturation rate} = \frac{(C_0 - C_t)}{C_0} \cdot 100\% \tag{4}$$

where z is the apparent charge number when an ion forms a stable structure. F is the Faraday constant (96 485 C mol^{-1}). C_0 and C_t (mol l^{-1}) represent the alkali concentration at times 0 and t, respectively. V_0 and V_t (L) correspond to the volume of the alkali solution at times 0 and t, respectively. N is the number of repetitive units in the BMED cell (4 in this study). t is the time (s) to complete the desaturation level. U (V) and I_t (A) represent the loading voltage and actual current of the BMED stack, respectively. M (kg mol^{-1}) represents the molar mass per unit NaOH.

2.2.3 Cost model and economic feasibility. EPA cost curves were used for the ion exchange process.[15] The Consumer Price Index factor for the years 1979–2025 (ref. 35) was applied to update the capital cost.

The costs of bipolar electrodialysis were estimated based on the total investment cost of the equipment. The equipment requirements were determined with the mass transfer requirements according to the desired conversion of salt input into acid and base. The mass transfer was estimated by transferring sodium moles from the salt compartment to the alkaline compartment, using a previously calibrated concentration and conductivity curve of the soda solution. The total capital cost was obtained from the equipment investment cost using previously published economic scaling models.[34]

For the economic analysis of BMED, the normalized energy consumption per kilogram of soda produced was considered. The total production cost of BMED can be defined as the sum of fixed, related to capital cost amortization, and operating costs (*e.g.*, energy and maintenance).[2]

$$C_{\mathrm{Pro,BMED}} = C_{\mathrm{fixed}} + C_{\mathrm{operating}} \tag{5}$$

The main parameters used in the cost model include the cost of the bipolar membrane (600 USD per m^2), the cation membrane (100 USD per m^2) and the anion membrane (100 USD per m^2), data that were discussed with different suppliers. In addition, the cost of energy was considered to be 45 USD per MWh.

On the other hand, the base case of analysis corresponds to concentrate evaporation and crystallization, evaluated using cost models obtained from the literature.[17] The cost was updated using the Consumer Price Index factor for the years 2008–2025. The technical capability of this equipment is well-validated even for the treatment of highly concentrated streams.[17] The cost model depends on the treatment flow rate and has different cases based on the salt concentration in the stream to be treated.

3. Results

3.1 Desaturation process

The influent of the treatment system is the tertiary effluent. Hardness ions are first removed by IX and the remaining ions by pEDR. The pEDR dilute stream serves as the recovered water for the pulp mill. Since IX capacity decreases at high salinity,[7] placing IX before pEDR optimizes performance and reduces regeneration chemical use, treating a lower salt concentration in the concentrate loop. This configuration was validated *via* WAVE simulations and improves both pEDR and BMED membrane performance and lifespan (Fig. 1).

Electrodialysis is designed for removal of small ions. Therefore, in this case it is also seen as a pretreatment and isolation stage for BMED, as it decreases the occurrence of organics in the concentrate. The subsequent treatment of this organic matter is critical for industrial implementation. One of the most promising technologies is electrochemical advanced oxidation with boron-doped diamond anodes.[30] BDD electrodes have been considered as an optimal electrode material due to their favourable physical and chemical properties. The feasibility of the EAOP with BDD for this application is robustly supported by studies demonstrating its efficiency in high salinity/conductive media, such as treatment of reverse osmosis concentrates and high-salinity industrial wastewater.[16] While detailed analysis of this specific downstream treatment is outside the scope of the present study, the literature confirms the BDD/EAOP pathway as an effective strategy for the complete oxidation of organic matter in the resulting concentrate.[16,30]

A fraction of the pEDR concentrate is recirculated, while the rest is desaturated in BMED. BMED dilute (Fig. 2) is only partially desalinated and recirculated back into a concentrate tank, which acts as a buffer. At steady state, the flow of ions from the dilute to the concentrate in pEDR is equal to the flow of ions that are converted into BMED products in the desaturation circuit. That is, the objective of the desaturation stage is to maintain a balanced ion transfer from the pEDR dilute into BMED products.

As mentioned above, the main salts identified in the concentrate are NaCl and Na_2SO_4. Therefore, the focus of BMED is to transform these salts into acid and base products. Regarding other elements, multivalent cations, mainly calcium and magnesium, were removed during pretreatment by ion exchange. These cations were subsequently transformed into sodium hydroxide and calcium carbonate through chemical precipitation from the IX regeneration stream, which was validated by modelling in PHREEQC. Moreover, potassium does not represent a problem for the BMED system, like sodium, it can be easily transferred to the alkaline compartment and transformed into potassium hydroxide.

For the industrial scale-up economic evaluations, a pulp mill effluent flow rate of 2500 m^3 h^{-1} was considered. Based on the input salts to BMED and the ion transfer from the dilute to the concentrate in pEDR, a mass balance estimation determined that for a feed flow rate of 200 m^3 h^{-1} in BMED, desaturation rates of 80%, 55%, and 45% were required for input conductivity levels of 10 mS cm^{-1}, 14 mS cm^{-1}, and 18 mS cm^{-1}, respectively. This transfer allows steady state operation between the desalination system and the desaturation system to be maintained. A higher desaturation rate is required for lower input concentrations to ensure the same mass transfer in all three cases. For practical purposes in the BMED experiments, the desaturation rate for the identified salts was considered equivalent to the percentage reduction in conductivity. Therefore, BMED was operated until the final conductivity of the salt compartment reached 2.00 mS cm^{-1}, 6.30 mS cm^{-1}, and 9.90 mS cm^{-1}, respectively.

3.2 Ion exchange column and chemical precipitation modelling

Sorption mechanisms depend on solid–liquid interactions and system conditions. Therefore, sorption capacity and required contact time are key parameters to assess.[3] Ion exchange (IX) is commonly studied through kinetics, equilibrium, and column operation experiments,[21] all of which apply models that describe adsorption or ion exchange processes. While batch studies offer valuable data, they are not directly applicable to continuous systems.[3] For this reason, fixed-bed column experiments were performed to gain practical operational insights.

The aim of the IX experiments was to determine the breakthrough point of resins treating real effluent. Breakthrough curves provide critical data for scaling up.[11] These curves were built by monitoring the effluent concentration as a function of the treated volume. Although 5% of the influent is a common definition for breakthrough, in this study, it was set at 10% due to the low inlet concentrations of calcium and magnesium. This corresponds to less than 1 mg L^{-1}, below the 5 mg L^{-1} threshold to avoid scaling in BMED.[12]

Fig. 3 shows the saturation curves for calcium and magnesium. Adsorption was effective, keeping calcium below 0.18 mg L^{-1} and magnesium below 0.05 mg L^{-1} in the effluent. As exchange sites are gradually occupied, concentrations increase until the resin exhaustion. However, the process was stopped before that point, focusing instead on the resin's capacity up to the predefined breakthrough.

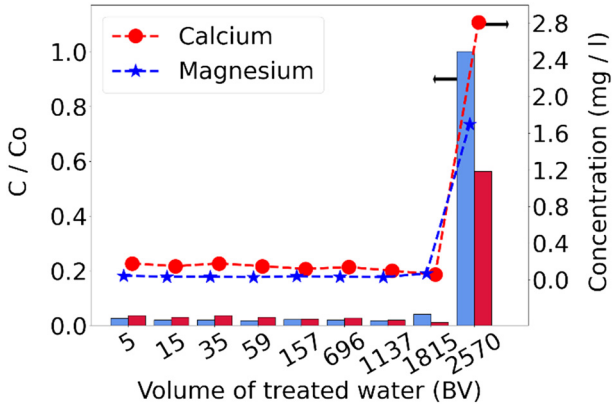

Fig. 3 Ion exchange effluent concentration for different volumes of treated effluent for magnesium (★) and calcium (●). Effluent concentration/initial concentration (C/C_o) for magnesium (left bar) and calcium (right bar) at different treated volumes.

The breakthrough was identified at the intersection between the data projection and the threshold line (C_{tb}). For calcium, it occurred at 1937 bed volumes (BV), and for magnesium at 1861 BV. Since magnesium broke through first, the resin's exchange capacity was calculated up to this point, resulting in 0.68 eq L^{-1}. The capacity was lower than that reported by the supplier; this could be due to organic fouling caused by humic and fulvic acids,[7] and to the breakthrough point defined based on magnesium concentration, meaning that the column did not reach its full capacity.

Weak acid resins have a high affinity for hardness ions, making regeneration with salt ineffective. Instead, diluted acid is used to regenerate the resin to its hydrogen form, leveraging its strong affinity for hydrogen ions. The conversion to the sodium form is then achieved by neutralization with diluted sodium hydroxide.[7]

The IX regeneration stream was modeled using WAVE software, with the effluent characterization from Table 1 and a selected weak acid resin. Regeneration was simulated using 4% HCl and 4% NaOH. Although the aim is to use BMED products for regeneration, only soda is suitable. The acid stream from BMED has a high sulfate content, which could cause calcium sulfate precipitation. To avoid this, the BMED acid stream must be diluted or replaced with HCl. For simplicity, regeneration with HCl was considered, allowing the BMED acid to be used elsewhere.

The regeneration stream obtained from WAVE contained 1898 mg l^{-1} Na^+, 1644 mg l^{-1} Ca^{2+}, 325 mg l^{-1} Mg^{2+}, 6058 mg l^{-1} Cl^-, and 285 mg l^{-1} SO_4^{2-}. This was entered into PHREEQC to model sequential reactions with NaOH and Na_2CO_3 up to 1.15 times stoichiometry as shown in Fig. 4. NaOH led to $Mg(OH)_2$(s) precipitation, reducing Mg^{2+} to 4.86 mg l^{-1}. Then, $CaCO_3$(s) formed, reducing Ca^{2+} to 5.21 mg l^{-1}. Depending on requirements, additional steps could enable further valorization. Magnesium may be used as a fertilizer, and calcium carbonate as a raw material in pulp mills.

3.3 BMED

3.3.1 Regression model and current efficiency analysis. A factorial design of experiments with two factors was employed. The factors were voltage (5 levels) and inlet salt concentration (3 levels), resulting in a total of 15 experiments. All experiments were performed in duplicate, and the average value obtained from both tests was considered. Finally, ordinary least squares (OLS) regression was used to determine the mathematical model that best fits the data.

The current efficiency results obtained from the experiments are shown in Table 4, along with the values adjusted by the regression model. The modeled values closely match those obtained in the experiments, with a maximum difference of 3.98%.

The regression model was applied using the least squares method, and the regression equation is shown in eqn (6), where V is the applied voltage, C is the feed salt conductivity and Ie (%) is the current efficiency.

$$\text{Ie (\%)} = -71.66 + 18.15{\cdot}C + 3.37{\cdot}V - 0.59{\cdot}C^2 - 0.10{\cdot}V^2 \quad (6)$$

The regression presented a good fit, confirmed by the R^2 value of 0.96 and the adjusted R^2 of 0.94. Although R^2 provides an estimate of the strength of the relationship between the model and the response variable, it does not constitute a formal hypothesis test. Additionally, if the Prob(F-statistics) is lower than the significance level, it can be concluded that the R^2 value is significantly different from zero. In this case, with Prob(F-statistics) = 1.12×10^{-6} and considering a commonly used significance level of 0.05, it can be stated that the regression model predicts the response variable better than the response mean. This same analysis can be applied to predict energy consumption and ion flux, which are key parameters for scaling up this process.

3.3.2 Effect of voltage and salt concentration. Fig. 5 shows the desaturation rate in BMED as a function of applied voltage for three salt concentrations. Each test continued until steady-state ion transfer in pEDR, with varying durations depending on the voltage and required desaturation. Voltage affects water dissociation, salt migration through ion exchange membranes, and Joule heating in the membrane stack.[20] Increasing voltage enhances ion flux by providing a stronger driving force, as electrochemical reactions are potential driven.[4,6] As seen in Fig. 5, higher voltage results in a greater desaturation rate at the same salt concentration. However, it also increases the current and energy consumption,[28] so balancing ion transfer efficiency with energy use is essential.

Higher voltage improves current efficiency and acid/base concentration but increases energy use and heat

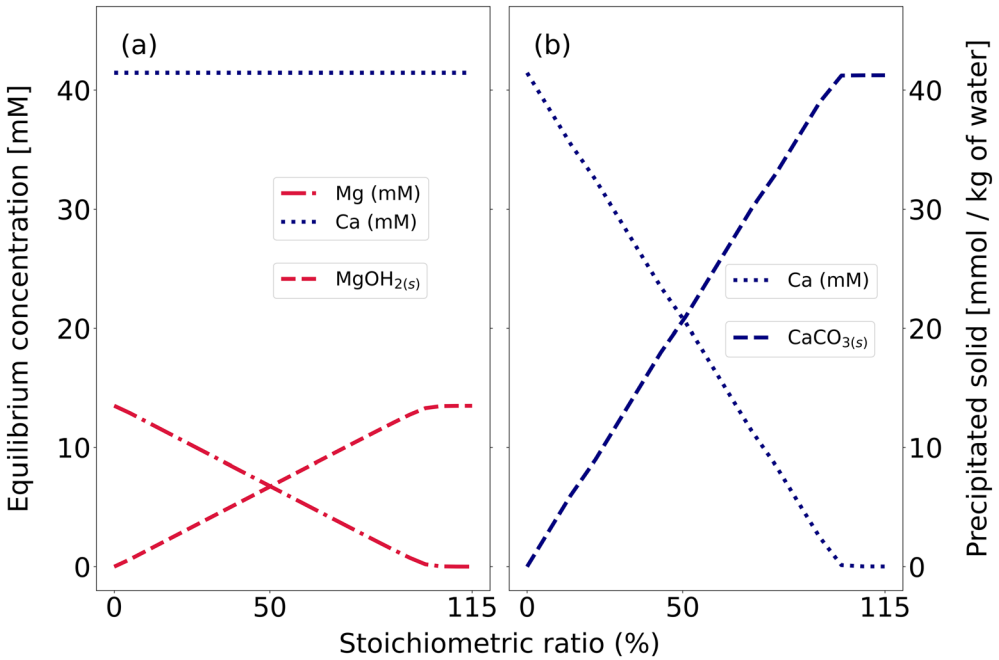

Fig. 4 Precipitation reaction of ion exchange regeneration stream in PHREEQC. (a) Concentration of calcium (▪ ▪) and magnesium (- ▪) after the reaction for different NaOH concentrations, also $MgOH_2$(s) (--) obtained from the reaction is observed. (b) Concentration of calcium (▪ ▪) after the reaction with Na_2CO_3 and $CaCO_3$(s) (--) obtained after the reaction.

Table 4 Experiment plan, obtained efficiency, predicted efficiency and residual values

Conductivity (mS cm^{-1})	Voltage (V)	Experimental Ie (%)	Model predicted Ie (%)	Residual (%)
10	14	78.70	78.38	0.32
10	16	79.05	79.08	−0.03
10	18	79.75	78.97	0.78
10	20	76.15	78.05	−1.90
10	22	93.70	94.44	−0.74
14	14	94.75	95.14	−0.39
14	16	95.40	95.03	0.37
14	18	94.65	94.11	0.54
14	20	90.40	91.66	−1.26
14	22	95.50	92.36	3.14
18	14	93.05	92.25	0.80
18	16	87.35	91.33	−3.98
18	18	77.15	76.32	0.83
18	20	92.60	92.38	0.22
18	22	90.90	89.60	1.30

generation, risking membrane damage.[20,41] Also note that while moderate voltage enhances demineralization, excessive levels cause energy losses and reduce membrane lifespan.

On the other hand, high demineralization rates lead to a higher resistance (lower conductivity) of the dilute compartment, decreasing the efficiency of the process in the long term. This can be observed in Fig. 6(a), where the energy efficiency improves progressively from 93.7% to 95.4% at 18 V but slightly decreases at 20 V (94.7%) and 22 V (92.6%). At 14 mS cm^{-1}, the peak efficiency occurs at 18 V, though differences across voltages are minimal. Thus, voltage selection should consider its overall impact on BMED costs, as analysed in later sections.

As the feed salt concentration increases, the membrane stack resistance decreases, allowing higher current density at constant voltage. Greater conductivity also lowers ohmic resistance, enhancing ion flux and H^+/OH^- generation. Fig. 6(b) shows that, at 18 V, the energy consumption per unit of soda decreases as the conductivity rises from 10 to 14 mS cm^{-1}, but it slightly increases at 18 mS cm^{-1}. This is due to higher salt concentrations raising current and energy use, generating more heat and potential losses. The efficiency also improves from 10 to 14 mS cm^{-1}, and then decreases beyond that point. Elevated salt concentrations increase osmotic pressure on the bipolar membrane, limiting H^+ and OH^- production from water dissociation.[20] Therefore, both voltage and feed concentration must be carefully optimized to

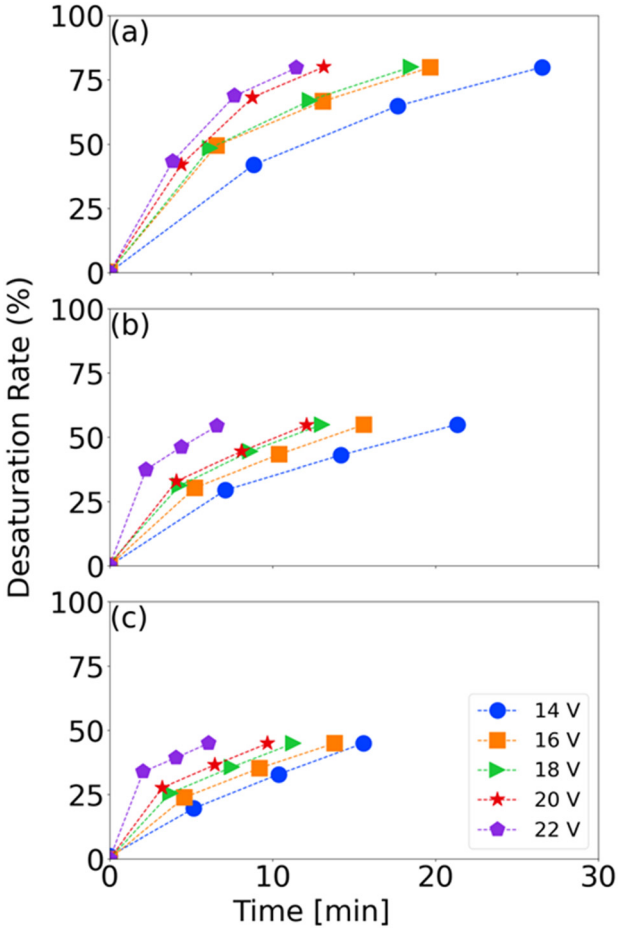

Fig. 5 Desaturation rate as a function of voltage for the case of (a) 10 mS cm^{-1}, (b) 14 mS cm^{-1} and (c) 18 mS cm^{-1}. Although the same amount of salts needs to be removed in all three cases, it is observed that as the salt concentration increases, the time required to reach the target decreases. Additionally, an increase in voltage leads to a higher desaturation rate.

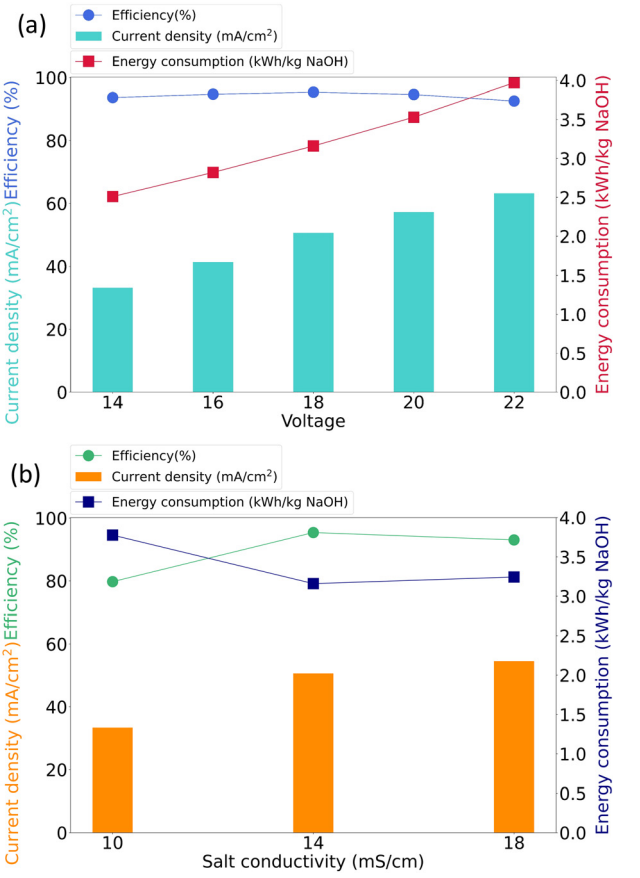

Fig. 6 (a) Effect of applied voltage on current efficiency, mean current density, and energy consumption for the 14 mS cm^{-1} case. (b) Effect of salt concentration on current efficiency, mean current density, and energy consumption for the 18 V case.

enhance BMED performance while minimizing energy consumption and membrane degradation.

3.3.3 Economic optimization of BMED. The previous analysis highlighted key factors for optimizing operating conditions while minimizing total costs, including capital and operational expenses. We preliminary ruled out evaluating a two-compartment configuration, as it has been reported to be less efficient, leading to higher membrane area and specific energy consumption requirements.[31] Therefore, different case studies based on a three-chamber configuration were assessed economically.

An initial evaluation was performed based on the feed salt concentration. As shown in Fig. 7(a), increasing salt concentration initially reduced the membrane area and energy consumption due to lower electrical resistance and improved mass transfer. However, beyond 14 mS cm^{-1}, further increases showed diminishing returns in the membrane area reduction and led to higher specific energy consumption.

Fig. 7(c) shows that increasing the conductivity from 14 to 18 mS cm^{-1} reduces capital costs, as higher current densities allow for a smaller membrane area. This benefit offsets the increase in energy consumption, resulting in a slightly lower total cost at 18 mS cm^{-1} (0.44 *vs.* 0.46 USD per kg NaOH). However, the cost difference is marginal. Additional factors must be considered when integrating the desaturation system with pEDR, such as water transport through membranes by osmosis and electroosmosis, which intensify with higher reject concentrations.[22] Considering these aspects, a feed salt concentration of 14 mS cm^{-1} was selected for further analysis on operating voltage.

Then, an economic analysis was conducted by setting the inlet salt concentration at 14 mS cm^{-1} and varying the operating voltage. As shown in Fig. 7(b), increasing the voltage reduces the required membrane area due to increased ion migration. However, it also can increase energy losses due to heat generation, decreasing energy efficiency and resulting in a near linear rise in energy consumption.

Fig. 7(d) shows the costs for the 14 mS cm^{-1} case as a function of operating voltage, normalized by the total

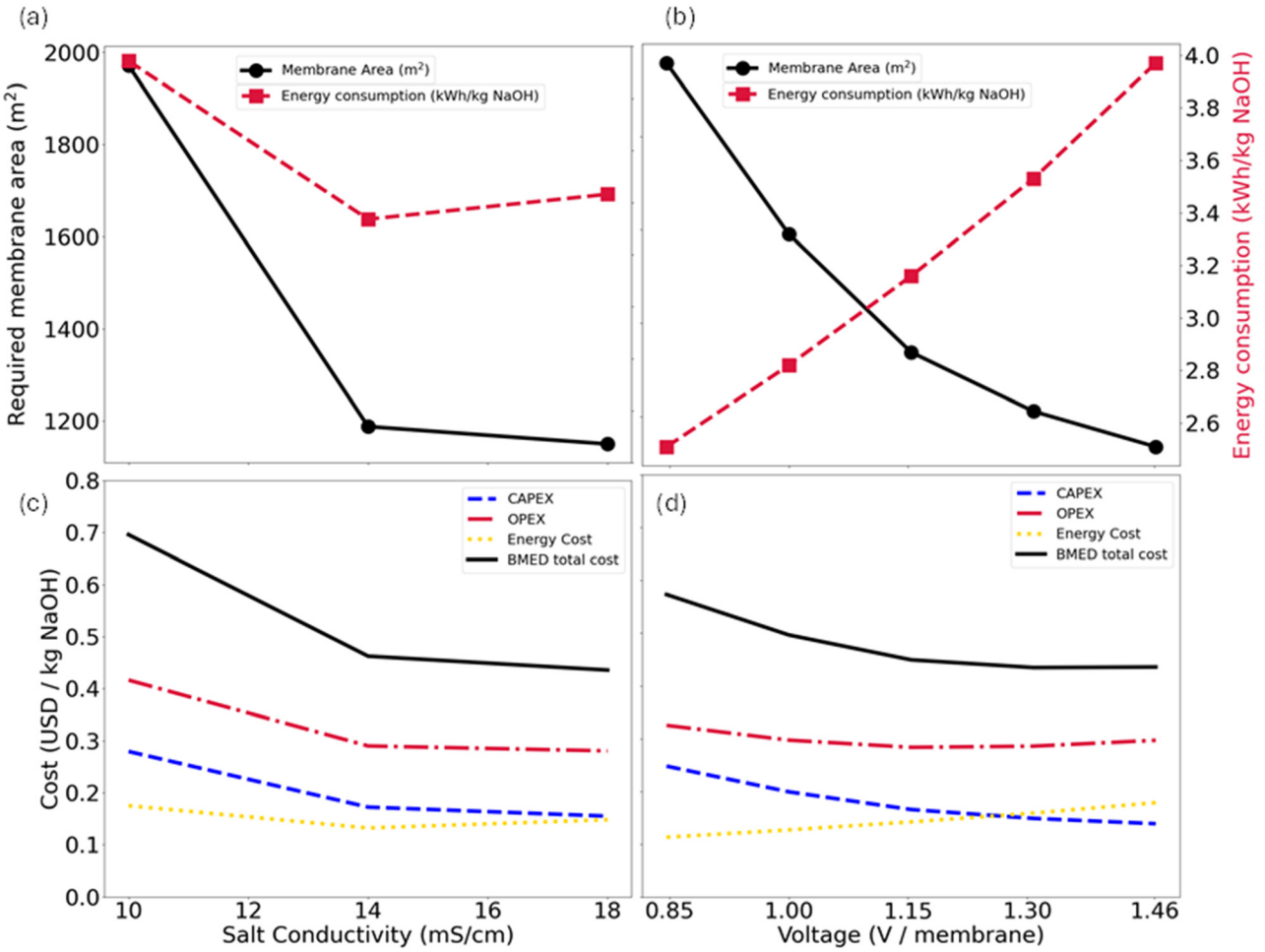

Fig. 7 Effect of feed salt concentration, expressed as conductivity, on (a) membrane area (m^2) and energy consumption (kWh kg^{-1} NaOH), and (c) BMED system costs normalized per kg of NaOH produced. Effect of voltage (V per membrane) on (b) membrane area (m^2) and energy consumption (kWh kg^{-1} NaOH), and (d) BMED system costs normalized per kg of NaOH produced.

number of membranes. Although increasing the voltage increases the energy cost, it reduces the capital cost by reducing the membrane area. This also decreases associated maintenance and replacement costs.

The total costs include all previously discussed factors. As the voltage increases, costs decrease from 0.57 USD per kg NaOH at 0.85 V per membrane to 0.43 USD per kg NaOH at 1.31 V per membrane. However, at 1.46 V per membrane, the total cost slightly increases to 0.44 USD per kg NaOH. This indicates that beyond 1.31 V per membrane, the rise in energy costs outweighs the reduction in capital expenses.

Preliminary tests at 1.62 V per membrane (24 V) reached 91.12 mA cm^{-2} at 14 mS cm^{-1}. This is impractical for semi-continuous operation, as acid and soda concentration increases reduce resistance and raise current, potentially exceeding the typical BMED range of 10–100 mA cm^{-2},[38] depending on the manufacturer. Therefore, the case of 14 mS cm^{-1} and 1.31 V per membrane (20 V) was selected for a semi-continuous experiment, representing a larger-scale operation.

3.3.4 Simulated scaling conditions in BMED experiments. Industrial conditions can be simulated at the lab scale through multistep experiments or by adjusting chamber volume ratios.[29] A multistep experiment was conducted by replacing the salt solution once the target conductivity was reached. Operating conditions were based on the economic optimization results: 14 mS cm^{-1} and 20 V. The goal was to evaluate process performance under conditions representative of pilot- or industrial-scale operation and use the results for economic analysis.

A nine-step experiment was performed, with the final step selected as the representative of industrial operation. In this stage, once acid and base concentrations reached target values, both streams operated in feed-and-bleed mode, purging some of the solution and adding make-up water to maintain stable concentrations.

The main parameters from the multistep experiment are shown in Fig. 8. The NaOH concentration reached 0.67 M. The efficiency in the final step was 73%, with an energy consumption of 4.57 kWh kg^{-1} NaOH. The NaOH flux achieved was 6.27×10^{-4} mmol cm^{-2} s^{-1}.

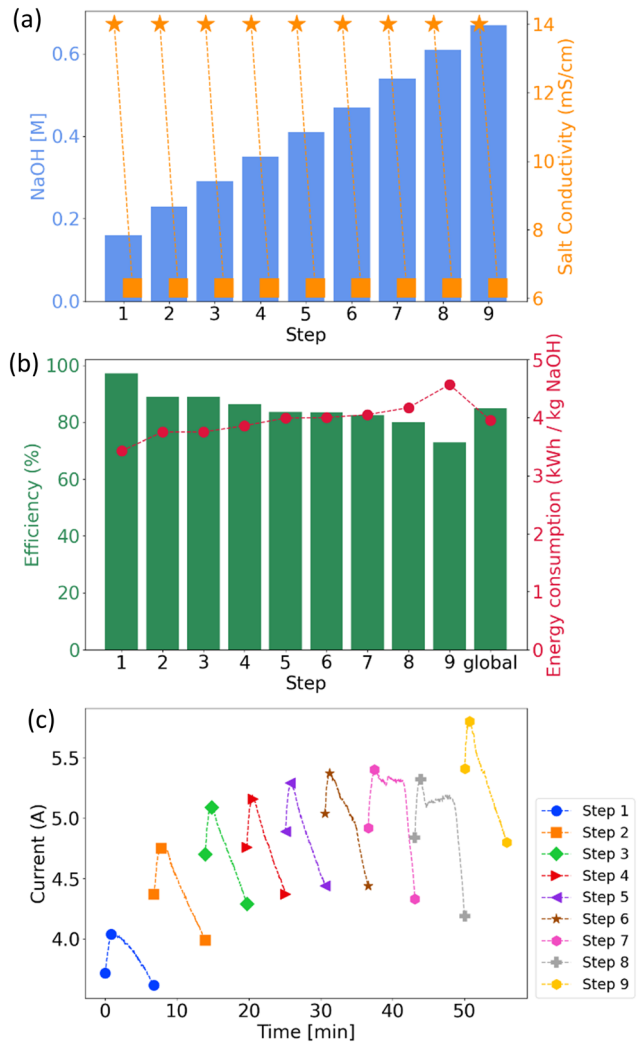

Fig. 8 Multistep BMED for the case of 14 mS cm^{-1} and 1.31 V per membrane. For each step, the following are shown: (a) initial (□) and final (■) conductivity in the salt compartment, as well as the NaOH concentration reached in each step (bar); (b) energy efficiency (bar) and energy consumption (●) of each step, along with the average across all steps (global); (c) current along each step.

The NaOH concentrations reached at each step, along with the initial and final conductivity of the saline compartment, are shown in Fig. 8(a). The initial conductivity was 14 mS cm^{-1}, and each step ended when it dropped to 6.30 mS cm^{-1}, achieving 55% desalination, required to maintain steady ion transfer in pEDR.

The current density increased from 60.63 mA cm^{-2} in the first step to 83.03 mA cm^{-2} in the final one, peaking at 90.63 mA cm^{-2}. This rise is due to the accumulation of acid and base, which lowers stack resistance. No additional stage was performed beyond this point to avoid exceeding the typical BMED upper limit (100 mA cm^{-2}), which causes membrane damage.[10] For sustainable long-term operations, a feed-and-bleed mode would maintain appropriate current density levels.

At each step, the current initially starts low due to high resistance from low acid/base concentrations. As concentrations rise, the resistance decreases, increasing the current. Then, as the salt solution becomes desaturated, the ion content drops, the resistance increases again, and the current decreases. This phenomenon has been previously observed by other researchers.[29,41]

The energy consumption rose from 3.43 to 4.57 kWh kg^{-1} NaOH across the steps, while the efficiency decreased from 97% to 73% (Fig. 8(b)). This is attributed to intensified H_3O^+ and OH^- leakage at higher concentrations, which reduces efficiency.[41] Additionally, higher osmotic pressure hinders water migration to the bipolar membrane interface, limiting H_3O^+ and OH^- generation.[40] Thus, lower initial acid/base concentrations favor lower energy consumption and higher efficiency compared to later stages.

3.4 Cost comparison with the conventional ZLD system

Using the parameters from the multistep operation, an economic evaluation of the proposed system was performed. The BMED design flowrate is 200 m^3 h^{-1}. Membrane costs were obtained from suppliers: 600 USD per m^2 for bipolar membranes and 100 USD per m^2 for ion exchange membranes.

For ion exchange (IX), the design flowrate is 2500 m^3 h^{-1}, corresponding to the effluent desalinated by pEDR. The chemical precipitation flowrate is 14 m^3 h^{-1}, based on the IX regeneration stream modeled with WAVE. The chemical precipitation evaluation includes chemical feed, rapid mixing, and sedimentation. A sludge drying or conditioning stage may be added depending on valorization needs and industry infrastructure.

Previous studies reported pEDR water recovery rates above 95%.[14] This study assumes 98% recovery to compare desaturation against a minimum-cost ZLD scenario. The evaporation and crystallization flowrate was

Table 5 Investment cost and operating cost of both systems, together with the main parameters used in the economic model

	CAPEX (USD)	OPEX (USD per year)
Desaturation system		
IX	$7 655 354	138 121
BMED	$10 978 554	2 530 618
CP	$1 798 518	182 062
Total	$20 432 425	2 850 800
Conventional ZLD		
Evaporation/crystallization	$28 179 167	$1 954 599
Solid disposal		$2 943 360
Total	$28 179 167	$4 897 959
Parameters		
BM	600	USD per m^2
CEM	100	USD per m^2
AEM	100	USD per m^2
Specific solid disposal cost	288	USD per ton
Energy cost	45	USD per MWh
Soda price for valorization	500	USD per ton

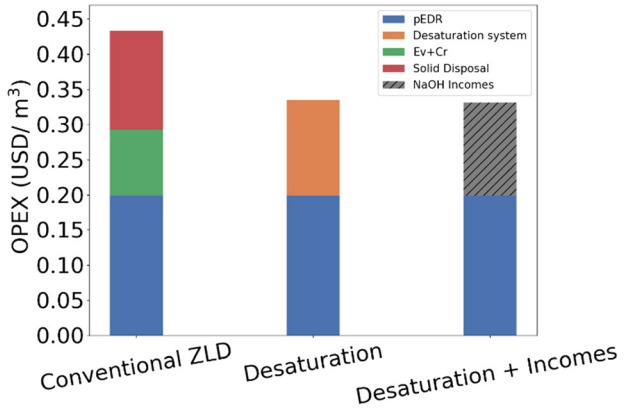

Fig. 9 OPEX comparison for both scenarios, including NaOH valorization (hatched line) in the third case.

set at 50 m^3 h^{-1} (2% of the effluent). ZLD systems typically generate a solid salt mixture that is difficult to valorize and is usually disposed of as waste. Therefore, landfill disposal costs were included.

Table 5 presents the disposal costs and main parameters of the cost model, along with estimated CAPEX and OPEX values for each process.

As shown in Table 5, the CAPEX of the evaporation/crystallization is about 38% higher than that of the desaturation system. Fig. 9 shows that the OPEX of the desaturation system is slightly higher than the OPEX of the conventional ZLD system. Although the specific energy consumption of the desaturation system (19 kWh m^{-3}) is lower than the evaporation and crystallization energy consumption (62.6 kWh m^{-3}), the higher flowrate of the BMED process explains the OPEX difference when normalized by the total treated water flow incorporating pEDR. However, the evaporation system requires the disposal of solids as waste, which has both a negative environmental impact and an additional cost. In contrast, the desaturation system considers the valorization of by-products, generating a positive impact on the overall cost balance.

Fig. 9 shows the OPEX for each stage, normalized per cubic meter of treated water (2500 m^3 h^{-1}). The OPEX of pEDR was estimated at 0.20 USD per m^3, the desaturation system (IX + BMED + CP) at 0.14 USD per m^3, and the conventional ZLD at 0.09 USD per m^3. Solid disposal in ZLD adds 0.14 USD per m^3. The desaturation system enables NaOH valorization, with a recovery of 5530 tons per year. At 500 USD per ton, this results in 2.77 MUSD per year. Accounting for this benefit, the combined OPEX of pEDR and desaturation drops to 0.20 USD per m^3, less than half of the 0.43 USD per m^3 for pEDR plus conventional ZLD with disposal. Additionally, desaturation reduces pEDR operating costs, as it avoids near-saturation conditions in the reject stream, lowering chemical use for pH and scaling control. This advantage may vary depending on the pEDR water recovery.

4. Conclusions

A techno-economic optimization of BMED was performed based on input voltage and salt concentration. The optimum conditions found were 14 mS cm^{-1} and 20 V. Under these conditions, a multistep operation was conducted to simulate industrial-scale performance, achieving 73% energy efficiency, 4.57 kWh kg^{-1} NaOH energy consumption, and a NaOH flux of 6.27×10^{-4} mmol cm^{-2} s^{-1}.

In IX, the breakthrough point was reached at 1861 BV, with an exchange capacity of 0.67 eq L^{-1}. Modeling confirmed the selective separation of calcium and magnesium *via* precipitation of calcium carbonate and magnesium hydroxide in the regeneration stream.

The desaturation system outperforms conventional ZLD in CAPEX, OPEX, and environmental impact. Validated through experiments (IX and BMED) and modeling (CP), the total OPEX is 0.34 USD per m^3, reduced to 0.20 USD per m^3 when accounting for soda valorization. In contrast, ZLD has a total cost of 0.43 USD per m^3.

The desaturation system addresses the issue of reject concentrate in desalination of pulp industry effluent with a holistic approach, solving the waste disposal problem by valorizing components in the wastewater stream. This approach could become the standard in the water and wastewater industry across different sectors, as regulations become more restrictive, and water becomes scarcer.

Next steps include evaluating organic fouling in BMED using real wastewater. While electrochemical advanced oxidation is proposed as an alternative for organic desaturation, its feasibility must be further assessed. Additionally, applying pulsed electric fields could enhance BMED performance and mitigate fouling.

Author contributors

L. Salas: writing – original draft, methodology, investigation, formal analysis. A. Schwarz: supervision, methodology, investigation, formal analysis. A. Gonzalez-Vogel: validation, supervision, resources, methodology, formal analysis, conceptualization.

Conflicts of interest

There are no conflicts of interest to declare.

Data availability

The data that support the findings of this study are available from the corresponding author upon reasonable request.

Acknowledgements

The authors are grateful to Arauco Bioforest SpA for funding this research and giving the rights to use the presented results.

References

1 M. Akhter, G. Habib and S. U. Qamar, Application of electrodialysis in waste water treatment and impact of fouling on process performance, *J. Membr. Sci. Technol.*, 2018, **8**(2), 1000182.

2 A. Basem, D. J. Jasim, P. Ghodratallah, S. AbdulAmeer, A. M. Mahmood and W. J. Khudhayer, *et al.*, Technical and financial feasibility of a chemicals recovery and energy and water production from a dairy wastewater treatment plant, *Sci. Rep.*, 2024, **14**(1), 11143.

3 L. Bibiano-Cruz, J. Garfias, J. Salas-García, R. Martel and H. Llanos, Batch and column test analyses for hardness removal using natural and homoionic clinoptilolite: breakthrough experiments and modeling, *Sust. Water Resour. Manag.*, 2016, **2**, 183–197.

4 J. C. Bui, K. R. M. Corpus, A. T. Bell and A. Z. Weber, On the nature of field-enhanced water dissociation in bipolar membranes, *J. Phys. Chem. C*, 2021, **125**(45), 24974–24987.

5 M. N. Cabrera, Pulp mill wastewater: characteristics and treatment, *Biol. Wastewater Treat. Resour. Recovery*, 2017, **2**, 119–139.

6 T. Chen, J. Bi, Y. Zhao, Z. Du, X. Guo and J. Yuan, *et al.*, Carbon dioxide capture coupled with magnesium utilization from seawater by bipolar membrane electrodialysis, *Sci. Total Environ.*, 2022, **820**, 153272.

7 Dow Water Solutions, Ion exchange resins Water Conditioning Manual, The Dow Chemical Company, Form No. 177-01766-1105.

8 Dupont, *Wave: Water application value engine (Version 1.82) [Software]*, Dupont Water Solutions, 2021.

9 Food and Agriculture Organization of the United Nations [Internet], [cited 2023 Mar 26], available from: http://www.fao.org/.

10 R. Fu, H. Wang, J. Yan, R. Li, B. Wang and C. Jiang, *et al.*, Ion injection bipolar membrane electrodialysis realizes over 8 mol/L NaOH conversion from a brine stream, *AIChE J.*, 2024, **70**(4), e18345.

11 D. Geraud, Ion Exchange Experiments – Water Softening and Deionization, *Bachelor thesis*, Williams Honors College, Honors Research Projects, 2016, p. 345, https://ideaexchange.uakron.edu/honors_research_projects/345.

12 K. Ghyselbrecht, M. Huygebaert, B. Van der Bruggen, R. Ballet, B. Meesschaert and L. Pinoy, Desalination of an industrial saline water with conventional and bipolar membrane electrodialysis, *Desalination*, 2013, **318**, 9–18, DOI: 10.1016/j.desal.2013.03.020.

13 A. Gonzalez-Vogel and O. J. Rojas, Exploiting electroconvective vortices in electrodialysis with high-frequency asymmetric bipolar pulses for desalination in overlimiting current regimes, *Desalination*, 2020, **474**, 114190.

14 A. Gonzalez-Vogel, J. J. Moltedo and O. J. Rojas, Desalination by pulsed electrodialysis reversal: Approaching fully closed-loop water systems in wood pulp mills, *J. Environ. Manage.*, 2021, **298**, 113518, DOI: 10.1016/j.jenvman.2021.113518.

15 R. Gumerman, R. Culp and S. Hansen, *Estimating Water Treatment Costs. Volume 2. Cost Curves Applicable to 1. WATER or Water Treatment Estimation Routine*, 1979, vol. 2, p. 542.

16 Y. He, H. Lin, Z. Guo, W. Zhang, H. Li and W. Huang, Recent developments and advances in boron-doped diamond electrodes for electrochemical oxidation of organic pollutants, *Sep. Purif. Technol.*, 2019, **212**, 802–821.

17 G. Juby, A. Zacheis, W. Shih, P. Ravishanker, B. Mortazavi and M. D. Nusser, Evaluation and selection of available processes for a zero-liquid discharge system for the Perris, California, Ground Water Basin (Desalination and Water Purification Research and Development Program Report No. 149), RECLAMATION Managing Water in the West, 2008.

18 A. Kiperstok and C. M. Silva, The responsibility of the pulp and paper sector with regard to sustainable development: how much is enough?, *Water Sci. Technol.*, 2007, **55**(6), 65–71.

19 Y. A. R. Lebron, V. R. Moreira and M. C. S. Amaral, Metallic ions recovery from membrane separation processes concentrate: A special look onto ion exchange resins, *Chem. Eng. J.*, 2021, **425**, 131812, DOI: 10.1016/j.cej.2021.131812.

20 Y. Liu, Y. Sun and Z. Peng, Evaluation of bipolar membrane electrodialysis for desalination of simulated salicylic acid wastewater, *Desalination*, 2022, **537**, 115866.

21 G. J. Millar, S. Papworth and S. J. Couperthwaite, Exploration of the fundamental equilibrium behaviour of calcium exchange with weak acid cation resins, *Desalination*, 2014, **351**, 27–36.

22 A. Moura Bernardes, M. A. Rodrigues and J. Z. Ferreira, General aspects of electrodialysis, in *Electrodialysis and Water Reuse: Novel Approaches*, Springer Berlin Heidelberg, Berlin, Heidelberg, 2013, pp. 11–23.

23 E. Nascimben Santos, C. M. Silva, J. L. Colodette, S. B. Z. de Almeida, A. J. V. Zanuncio and T. O. de Souza, *et al.*, Recirculation of treated effluent in the bleaching of kraft pulp, *BioResources*, 2020, **15**(4), 8944–8964.

24 National Council for Air and Stream Improvement (NCASI), Environmental footprint comparison tool, A tool for understanding environmental decisions related to the pulp and paper industry, Washington, D.C., 2009.

25 R. Pärnamäe, S. Mareev, V. Nikonenko, S. Melnikov, N. Sheldeshov and V. Zabolotskii, *et al.*, Bipolar membranes: A review on principles, latest developments, and applications, *J. Membr. Sci.*, 2021, **617**, 118538.

26 E. Pehlivan and T. Altun, The study of various parameters affecting the ion exchange of Cu^{2+}, Zn^{2+}, Ni^{2+}, Cd^{2+}, and Pb^{2+} from aqueous solution on Dowex 50W synthetic resin, *J. Hazard. Mater.*, 2006, **134**(1–3), 149–156.

27 Y. Qiu, S. Wu, L. Xia, L. F. Ren, J. Shao and J. Shen, *et al.*, Ionic resource recovery for carbon neutral papermaking wastewater reclamation by a chemical self-sufficiency zero liquid discharge system, *Water Res.*, 2023, **229**, 119451.
28 D. Reeve and C. M. Silva, Closed cycle systems for manufacture of bleached chemical wood pulp, *Chemical pulping*, 2000(6), 440–473.
29 H. Ruan, S. Wu, X. Chen, J. Zou, J. Liao and H. Cui, *et al.*, Capturing CO_2 with NaOH solution from reject brine via an integrated technology based on bipolar membrane electrodialysis and hollow fiber membrane contactor, *Chem. Eng. J.*, 2022, **450**, 138095.
30 C. Salazar, I. Sirés, R. Salazar, H. D. Mansilla and C. A. Zaror, Treatment of cellulose bleaching effluents and their filtration permeates by anodic oxidation with H_2O_2 production, *J. Chem. Technol. Biotechnol.*, 2015, **90**(11), 2017–2026.
31 A. Schwarz, L. Salas, I. Nancucheo and A. González-Vogel, Zero liquid discharge recovery system for maximized tailings water reuse, *J. Environ. Manage.*, 2025, **394**, 127272.
32 J. Shen, J. Huang, L. Liu, W. Ye, J. Lin and B. Van der Bruggen, The use of BMED for glyphosate recovery from glyphosate neutralization liquor in view of zero discharge, *J. Hazard. Mater.*, 2013, **260**, 660–667, DOI: 10.1016/J.JHAZMAT.2013.06.028.
33 H. Tang, X. Wang, X. Zhao, Y. Dong, B. Xu and L. Wang, Ion migration characteristics during the bipolar membrane electrodialysis treatment of concentrated reverse osmosis brine, *Desalination*, 2023, **561**, 116660.
34 R. Thompson, M. Paleologou and R. M. Berry, Caustic soda and sulfuric acid production from sodium sulfate by-product of chlorine dioxide generation - economics, *Tappi J.*, 1995, **78**(6), 127–134.
35 U.S. Bureau of Labor Statistics [Internet], [cited 2023 Dec], available from: https://www.bls.gov/.
36 U.S. Geological Survey, *PHREEQC (Version 3) [Software]*, 2021, available from: https://www.usgs.gov/software/phreeqc-version-3.
37 F. Vassallo, D. La Corte, N. Cancilla, A. Tamburini, M. Bevacqua and A. Cipollina, *et al.*, A pilot-plant for the selective recovery of magnesium and calcium from waste brines, *Desalination*, 2021, **517**, 115231.
38 G. Virruso, C. Cassaro, A. Culcasi, A. Cipollina, A. Tamburini and I. D. L. Bogle, *et al.*, Multi-scale modelling of an electrodialysis with bipolar membranes pilot plant and economic evaluation of its potential, *Desalination*, 2024, **583**, 117724.
39 Y. Wang, X. Zhang and T. Xu, Integration of conventional electrodialysis and electrodialysis with bipolar membranes for production of organic acids, *J. Membr. Sci.*, 2010, **365**(1–2), 294–301.
40 Y. Wei, Y. Wang, X. Zhang and T. Xu, Treatment of simulated brominated butyl rubber wastewater by bipolar membrane electrodialysis, *Sep. Purif. Technol.*, 2011, **80**(2), 196–201.
41 H. R. Yang, B. Li, C. Q. Zhang, J. C. Yang, Y. M. Zheng and M. Younas, *et al.*, Bipolar membrane electrodialysis for sustainable utilization of inorganic salts from the reverse osmosis concentration of real landfill leachate, *Sep. Purif. Technol.*, 2023, **308**, 122898.
42 C. Yu, *Development and application of new electrodialysis technologies*, 2021.
43 X. Zhang, C. Ye, K. Pi, J. Huang, M. Xia and A. R. Gerson, Sustainable treatment of desulfurization wastewater by ion exchange and bipolar membrane electrodialysis hybrid technology, *Sep. Purif. Technol.*, 2019, **211**, 330–339, DOI: 10.1016/j.seppur.2018.10.003.